# Label-Free Probing of G-Quadruplex Formation by Surface-Enhanced Raman Scattering

**ARTICLE** *in* ANALYTICAL CHEMISTRY · AUGUST 2011

Impact Factor: 5.64 · DOI: 10.1021/ac201783h · Source: PubMed

analytical chemistry

ARTICLE

pubs.acs.org/ac

# Label-Free Probing of G-Quadruplex Formation by Surface-Enhanced Raman Scattering

Giulia Rusciano,[*,†] Anna Chiara De Luca,[‡] Giuseppe Pesce,[†] Antonio Sasso,[†] Giorgia Oliviero,[*,§] Jussara Amato,[§] Nicola Borbone,[§] Stefano D'Errico,[§] Vincenzo Piccialli,[⊥] Gennaro Piccialli,[§] and Luciano Mayol[§]

[†]Dipartimento di Scienze Fisiche, Complesso Universitario, Universitá di Napoli Federico II, Monte S. Angelo, Via Cinthia, I-80126 Napoli, Italy

[‡]SUPA—School of Physics and Astronomy, University of St. Andrews, North Haugh, KY16 9SS St. Andrews, U.K.

[§]Dipartimento di Chimica delle Sostanze Naturali, Universitá di Napoli Federico II, Via D. Montesano 49, I-80131 Napoli, Italy

[⊥]Dipartimento di Chimica Organica e Biochimica, Universitá di Napoli Federico II, Via Cinthia, I-80126 Napoli, Italy

Supporting Information

**ABSTRACT:** In this work, we establish the use of surface-enhanced Raman scattering (SERS) as a label-free analytical technique for the direct detection of G-quadruplex formation. In particular, we demonstrate that SERS analysis allows the evaluation of the relative stability of G quadruplexes that differ for the number of G tetrads and investigate several structural features of quadruplexes, such as the orientation of glycosidic bonds, the identification of distortions in the sugar−phosphate backbone, and the degree of hydrogen-bond solvation. Herein, the fluctuation of the SERS spectra, due to the specific interaction of vibrational modes with the SERS-active substrate, is quantitatively analyzed before and after quadruplex formation. The results of this study suggest a perpendicular orientation of the quadruplexes (with or without the 3′-tetra end linker) with respect to the silver colloidal surface, which opens new perspectives for the use of SERS as a label-free analytical tool for the study of the binding mode between quadruplexes and their ligands.

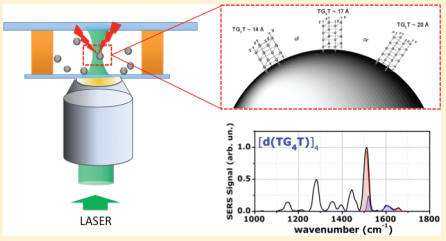


Nucleic acids are biomolecules characterized by a high extent of polymorphism, being able to fold into a number of different structures. Some of these are formed by guanine-rich oligodeoxyribonucleotides (GROs), which are able to form quadruplex structures. The building block of these unusual structures is the G tetrad. This consists of a planar arrangement of four guanine bases held together by a cyclic array of hydrogen bonds in which each guanine base both accepts and donates two hydrogen bonds. The importance of DNA quadruplexes resides in the relative abundance of GRO sequences in biologically important domains of the genome, such as, for instance, telomeres, specific regions codifying for immunoglobulins, gene promoters, and sequences involved in several human diseases.[1,2] Defects in such regions can cause mistakes in replication, transcription, or DNA recombination, thus enhancing cellular senescence and/or tumor proliferation. Recently, an important study on the human telomere appeared in the literature, demonstrating the existence of G-quadruplex structures in vivo.[3] Moreover, a number of investigations have proven that quadruplex structures are present in the scaffold of several oligonucleotides (aptamers) that are selectively recognized by proteins, such as TGP,[4] HIV gp120,[5] and thrombin.[6]

In this frame, there is a crucial requirement for the development of reliable, fast, and cheap experimental techniques and methodologies to monitor the formation of and to characterize the structure of G quadruplexes. Nuclear magnetic resonance, X-ray crystallography, circular dichroism (CD), and fluorescence assays are well-consolidated techniques for these purposes and in the past decade have greatly increased the understanding of G-quadruplex structures and their interaction with various drugs.[6,7] Raman spectroscopy is also a powerful analytical tool for the structural analysis of macromolecules such as DNA.[8,9] In particular, it has successfully been applied to probing of the phosphodiester backbone conformation, the sugar pucker, the glycosyl bond conformation, and the hydrogen-bonding interactions of DNA quadruplexes.[10] In particular, specific Raman markers have been identified as diagnostic of parallel and antiparallel G quadruplexes,[11] as well as for the anti or syn configuration of guanosine residues.[12] However, the effectiveness in applying Raman analysis has been limited by the relatively lower cross section of the Raman scattering process (typically on the order of $10^{-29}$ cm$^2$/molecule) compared to that of other spectroscopic processes, such as absorption and fluorescence

**Received:** July 11, 2011
**Accepted:** July 22, 2011
**Published:** July 22, 2011

($10^{-20}$ and $10^{-21}$ cm$^2$/molecule, respectively, in the visible region).

Surface-enhanced Raman scattering (SERS) has recently emerged as a technique suitable for overcoming the difficulties of low Raman cross sections.[13] Since its discovery in 1977, SERS has received a huge interest from researchers in many fields because of its high sensitivity and the minimal required sample volume, making it an ideal tool for the investigation of precious biological samples. The high sensitivity of this technique derives from the spectacular enhancement of the Raman cross section when the analyte is close to metallic (typically silver or gold) nanostructures. An enhancement factor up to 14 orders of magnitude has been reported for selected analytes such as Rd6G or crystal violet molecules.[14] In this regime, it is possible to detect the Raman signal even from single molecules. However, the enhancement is usually limited to 5−6 orders of magnitude for other molecules, which, nevertheless, allows Raman determination of a sample concentration in the micromolar regime. The metallic surface (SERS-active substrate) is usually in the form of a thin layer of metallic film or a suspension of aqueous metallic colloidal nanoparticles. The direct detection of DNA bases or short DNA sequences at low concentration has recently been reported in several studies. In particular, Kneipp and co-workers have demonstrated effective SERS cross sections on the order of $10^{-16}$ cm$^2$/molecule for adenine base, which allowed base investigations in the single-molecule regime.[15] Recently, Hu et al. have demonstrated the possibility of the sensitive detection of nucleic acids, down to the picomolar level, by combining rolling-circle amplification with SERS spectroscopy.[16] A model paramagnetic nanoparticle assay has also been demonstrated for the SERS detection of DNA oligonucleotides.[17]

However, the detection of DNA structures is more difficult because of the well-known dependence of the Raman scattering enhancement from orientation of the DNA with respect to the SERS-active substrate.[18] Nonetheless, in these conditions, even if SERS analysis in the single-molecule regime becomes prohibitive, it still remains a useful analytical approach for investigating DNA structures. In 2003, Breuzard et al. demonstrated that SERS can be used to test oligonucleotide stabilization in quadruplex structures.[19] In this case, the authors monitored the SERS signal from ethidium bromide, which, bound to quadruplex-conformed oligonucleotides, decreases up to a factor of 15, while no direct contribution from nucleic acids was observed.

In this paper, we show for the first time that direct SERS analysis can be employed to gain insight into the structural arrangement of G-rich DNA sequences prone to quadruplex formation. We demonstrate, for the first time, that SERS can be used to analyze the relative stability of G-quadruplex structures with different numbers of G planes. In particular, specific Raman features specific to quadruplex arrangement are identified in the spectra of different DNA sequences, and their relationship to the strength of Hoogsteen-type hydrogen bonding and phosphodiester backbone conformation is evaluated. The problem of intrinsic fluctuations of SERS spectra is also discussed. Our experimental outcomes demonstrate that the transition of single DNA strands to quadruplex structures greatly improves the reproducibility of the SERS spectra in terms of the relative intensity of the various Raman features. The analysis suggests that, after the formation of quadruplex structures, DNA tends to adopt a "standing-up orientation", exposing the G tetrad to the surface. This preferential orientation direction promotes the enhancement of Raman bands corresponding to intrastrand bonds, which constitutes an evident positive feature when investigating the formation of G quadruplexes. Finally, a further step of this study is devoted to the investigation of newly developed tetra-end-linked oligodeoxynucleotide (TEL-ODN) structures. These structures, constituted by four ODN strands, whose 3′-ends are attached to a non-nucleotidic branched tetra end linker, form more stable parallel G quadruplexes compared to the corresponding tetramolecular structures. The analysis reported in our paper provides further insight into their structural arrangement, in relation to two specific lengths of linker residues (long L and short S).

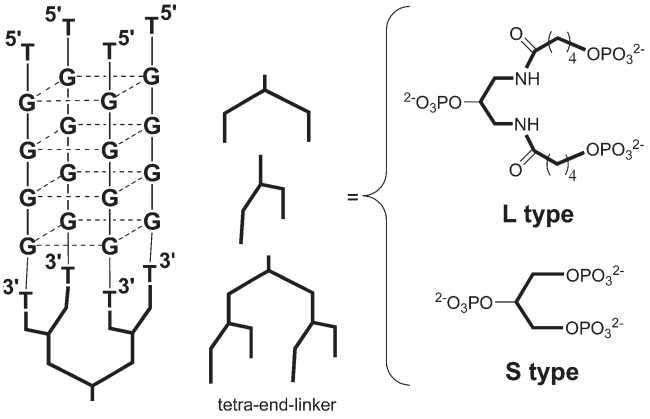


**Figure 1.** Schematic structures of the investigated TEL-ODNs *L*-$(TG_4T)_4$ and *S*-$(TG_4T)_4$.

## EXPERIMENTAL SECTION

**Synthesis of DNA and the Formation of G-Quadruplex Structures.** The synthesis of unmodified oligodeoxynucleotides (ODNs) was performed using standard phosphoramidite chemistry on controlled pore glass supports using an Expedite 8909 DNA synthesizer (15 $\mu$ mol; Applied Biosystems). The synthesis of tetra-end-linked ODNs (TEL-ODNs), *L*-$(TG_4T)_4$ and *S*-$(TG_4T)_4$, was performed according to the previously described procedure,[20,21] as shown in Figure 1. More details can be found in the Supporting Information.

**SERS Analysis.** SERS analyses were performed by using a home-built system based on an inverted microscope endowed with a Raman probe at 532 nm (Spectra Physics, Millennia Xs).[22] More details are provided as Supporting Information. To perform SERS measurements, an aliquot of a silver colloidal solution was added to the sample. The silver colloids that formed the SERS-active substrate were prepared according to the standard procedure of Lee and Meisel.[23] Briefly, $AgNO_3$ (90 mg) was dissolved in 500 mL of $H_2O$ and brought to boil. A sodium citrate solution (10 mL, 1%) was added under vigorous stirring. The solution was kept boiling for 1 h. Before use, the silver solution was diluted appropriately with distilled water.

## MEASUREMENTS AND ANALYSIS

**CD and CD Melting Measurements.** CD spectra were acquired to examine ODNs folding into a parallel or antiparallel conformation. Spectra were measured using a Jasco J-715 spectropolarimeter equipped with a Jasco JPT-23-S temperature controller. More details are reported as Supporting Information. Parallel quadruplexes display a positive Cotton effect at around 265 nm and a negative Cotton effect at 240 nm, whereas antiparallel ones exhibit

**Table 1. CD Signatures and $T_m$ Values of DNA Sequences Used in This Study**

| | CD signatures (nm) | | |
|---|---|---|---|
| sequence | CD (+) positive effect | CD (−) negative effect | $T_m$ values (°C) |
| d($TG_3T$) | 263 | 239 | 55.1 ± 0.1 |
| d($TG_4T$) | 264 | 240 | >90 |
| d($TG_5T$) | 264 | 240 | >90 |
| d(CTGTGTT) | N.O.[a] | N.O.[a] | N.O.[a] |
| *L*-($TG_4T$)$_4$ | 264 | 240 | >90 |
| *S*-($TG_4T$)$_4$ | 264 | 240 | >90 |

[a] N.O.: not observed.

a positive Cotton effect at around 295 nm and a negative Cotton effect or shoulder at around 260 nm. CD spectral analysis of investigated ODN samples, annealed in a 100 mM potassium buffer, showed typical profiles of parallel G-quadruplex arrangement, except in the case of d(CTGTGTT) (Table 1).

**Analysis of SERS Spectral Fluctuations.** As is well-known, in the single-molecule regime, a sequence of acquired SERS spectra from a supposed homogeneous sample produces strong fluctuations in both the band position and peak intensity. Intensity fluctuations arise from both the blinking effect[24] and the fluctuation in the number of "hot sites" (where the electromagnetic enhancement is particularly high) within the Raman confocal volume.[17,25] Furthermore, the relative intensities of the spectral features in SERS analyses are expected to differ significantly from those in normal Raman spectra, owing to specific surface selection rules.[26] In particular, only vibrations involving atoms close to the silver surface will be enhanced. For instance, it is easy to understand that the out-of-plane bending modes of a molecule flat-adsorbed on the metallic SERS substrate will be enhanced when compared with its in-plane bending modes, and vice versa in the case of a perpendicular orientation with respect to the surface.[27,28] At the same time, the vibrational modes of groups directly interacting with the metal surface may undergo a consistent wavenumber shift (on the order of tens of reciprocal centimeters) in SERS spectra with respect to spontaneous Raman scattering due to a chemisorption process.[29,30] All of these surface-induced effects can sometimes make it difficult to use as a reliable strategy for the label-free detection of biomolecules such as DNA. Recently, huge efforts have been made to develop new methodologies and substrates for obtaining sensitive and reproducible SERS signals of DNA sequences.[18] As a general rule, it has been observed that SERS signals are strongly dependent on both the sequence composition and structure. For instance, Gearheart et al. found that some assigned dsDNA sequences show acceptable SERS signals, while none of the corresponding ssDNA oligomers can be detected under the same experimental conditions.[31] Contrary to this, it has also been reported that the SERS spectrum of single-stranded calf thymus DNA is much stronger than that of the double-stranded sequence.[32] Although this strong dependence of the SERS efficiency on the DNA structure is certainly, for some applications, an unfavorable feature, at the same time, it can provide a useful feature for analysis of the conformational state of DNA strands and the changes induced by external agents (temperature, salt addition, etc.). The work presented herein explores

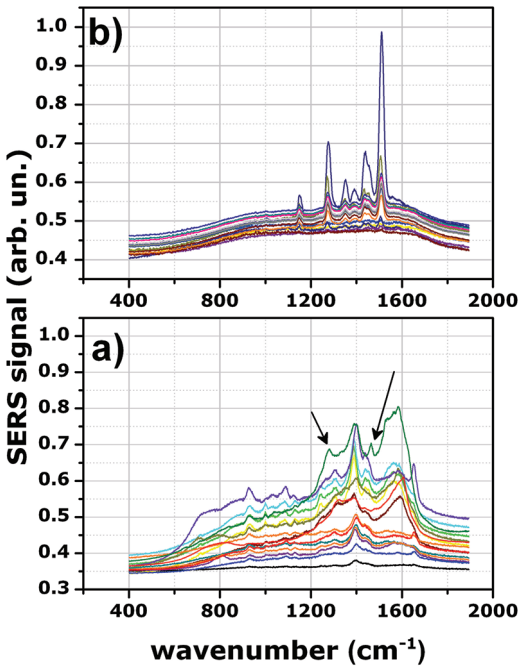


**Figure 2.** 20 randomly selected SERS acquisitions (raw data) for d($TG_4T$) samples, at a concentration of $10^{-5}$ M, in aqueous solution (part a) and in a $K^+$ buffer (part b). The two arrows indicate two peaks that are widely shifted with respect to the other acquisitions.

the potential to monitor the degree of quadruplex structures for assigned DNA sequences.

A significant difference between unstructured ODN bases and G-quadruplex DNA was observed, and it is worth noting the reproducibility of the acquired SERS signals. Figure 2 compares 20 successive SERS acquisitions for d($TG_4T$) samples at a concentration of $10^{-5}$ M both in pure water (part a) and in a $K^+$ buffer (part b). In both cases, no spontaneous Raman scattering signals can be detected. Significant variations in the SERS spectra of part a, in terms of both the signal intensity and relative Raman peak intensities, can easily be observed, although many features common to most of the spectra can be recognized. Excluding minimal effects due to the presence of the sample of unpaired bases and strain fragments, these data suggest a random orientation and proximity of DNA strands to silver colloids. This hypothesis seems to be confirmed by the slight but evident relative shift of the Raman peaks, which are common to most of the acquired SERS spectra. In Figure 2, it can be noted that that the wider spectral shifts can be observed for peaks that appear to be strongly enhanced. For instance, this is the case of the peaks around 1280 and 1467 $cm^{-1}$ of the spectrum colored in green in Figure 2 (part a), which appear to be shifted by more than 20 $cm^{-1}$ with respect to the other acquisitions. The peak shift induced by the SERS effect could also explain the broad spectral feature around 1580 $cm^{-1}$, which likely arises from spectral averaging between adjacent peaks. After the formation of G quadruplexes, the d($TG_4T$) SERS spectra appear dramatically different and highly reproducible, in terms of the relative amplitude of the different Raman features (part b of Figure 2). It is worth noticing that the reproducibility of these measurements was tested by comparing the spectra obtained on different days and on different sample batches. Notably, a clear improvement in the reproducibility of the SERS signals was observed for

all other DNA strands after quadruplex formation. A quantitative description of this effect can be obtained by evaluating, for the two samples, the Euclidean distance (ED) of each spectrum, described by the vector $S = (y_1, y_2, \ldots y_N)$, with respect to the average spectrum $S = (\bar{y}_1, \bar{y}_2, \ldots, \bar{y}_N)$, according to the relation

$$\mathrm{ED} = \sum_{i=1}^{N} (y_i - \bar{y}_i)^2 \qquad (1)$$

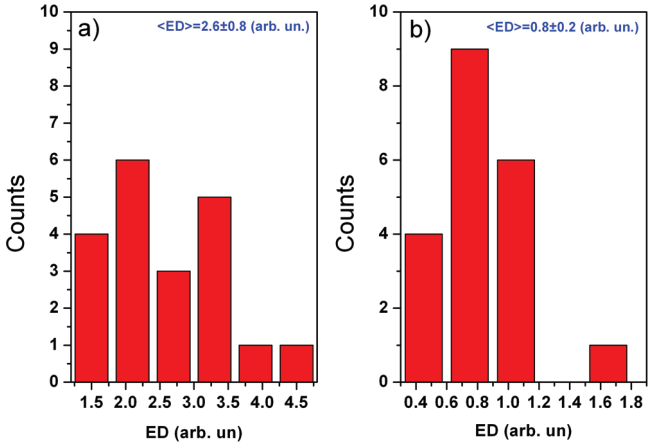


**Figure 3.** ED value distributions for d($TG_4T$) in $H_2O$ (a) and a $K^+$ buffer (b).

This parameter can be used to evaluate the "proximity" of different spectra.[33] In our case, it is used to estimate the distance of spectra with respect to the average spectrum, in order to highlight the variation in the reproducibility of the signals before and after the quadruplex restructuring.

We have evaluated the ED for all d(TG4T) spectra in Figure 2, after baseline subtraction and normalization to the most prominent spectral feature. The results are arranged in the frequency plots of Figure 3. As is possible to see, the higher signal reproducibility observed after quadruplex formation is mirrored by a mean ED value, equal to 0.8 ± 0.2 arbitrary units, that is much closer to the ideal case of perfect reproducibility (⟨ED⟩ = 0 arbitrary units) with respect to the single-stranded sample, where ⟨ED⟩ = 2.6 ± 0.8 arbitrary units.

**SERS Characterization of d($TG_nT$) ($n = 3-5$) and d(CTGTGTT) Samples.** Figure 4, left side, reports the SERS spectra, between 800 and 1700 $cm^{-1}$, for d($TG_nT$) ($n = 3-5$) strands in aqueous solution. The assignments of the main features are reported in Tables 2 and 3.

Measurements were taken on samples of 0.5 $\mu$M DNA concentration. Under these conditions, it is possible to estimate the number of molecules in the confocal detection volume (~0.5 fL), on the order of 1000 for all analyzed samples. Each spectrum in Figure 4 derives from 50 acquisitions in different SERS-active sites, each obtained with an integration time of 10 s.

Spectra showing no significant features were removed, while the remaining acquisitions were summed to provide an average spectrum. This procedure leads to a significant reduction in, if

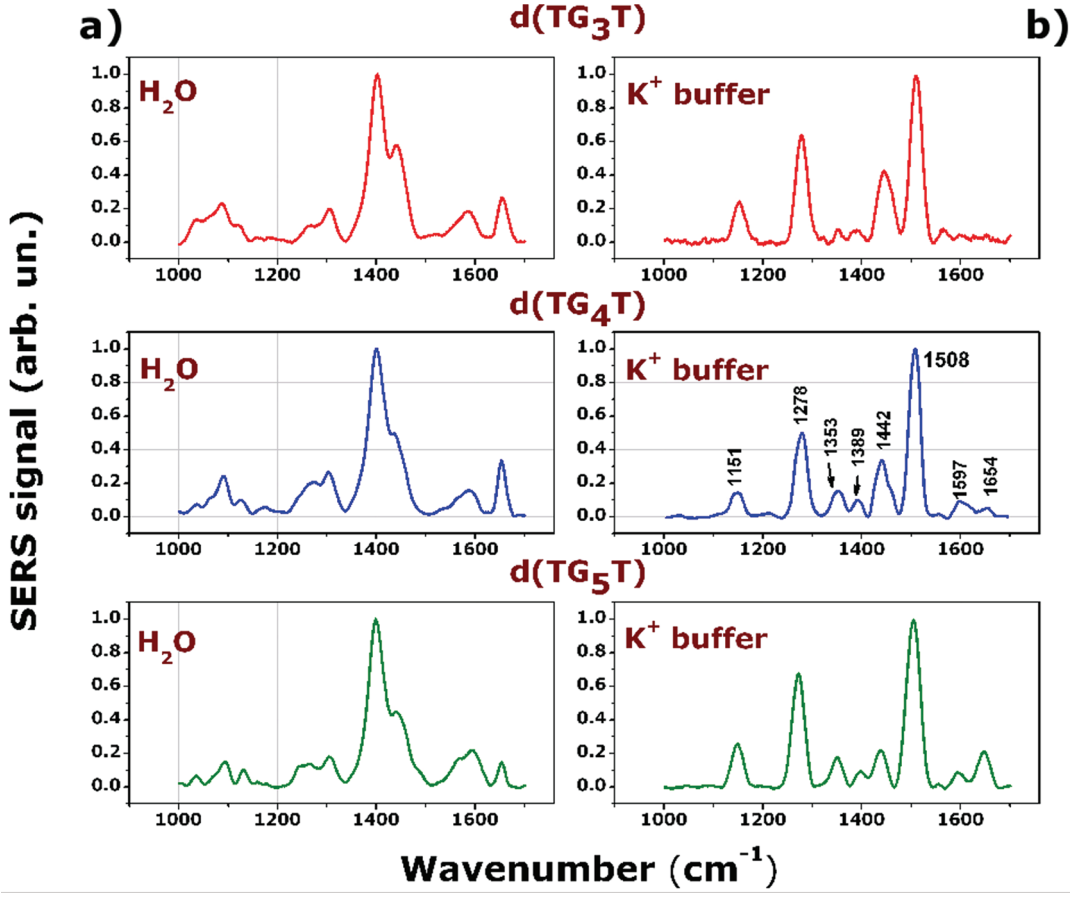


**Figure 4.** SERS spectra of selected oligonucleotides analyzed in this work in the region between 800 and 1700 $cm^{-1}$ both in $H_2O$ (a) and in a $K^+$ buffer (b). All of the samples were at a $5 \times 10^{-6}$ M concentration.


dx.doi.org/10.1021/ac201783h |Anal. Chem. 2011, 83, 6849–6855

**Table 2. Spectral Assignment for the Most Prominent SERS Features for DNA Strands in $H_2O$**

| SERS shift ($cm^{-1}$) $d(TG_3T)$/ $d(TG_4T)$/$d(TG_5T)$ | Raman shift ($cm^{-1}$) | assignment | refs |
|---|---|---|---|
| 1036/1036/1036 | 1020 | dG, N−H | 34 |
| 1086/1086/1092 | 1082 | $PO^-_2$ | 34 |
| 1125/1125/1130 | 1120 | unpaired dT (N3) | 10 |
| 1267/1270/1268 | 1238 | dT (N3) | 10 |
| 1304/1304/1303 | | unassigned | |
| 1401/1399/1399 | 1417 | d | 9 |
| 1440/1437/1441 | 1423 | deoxyribosyl (C5′$H_2$) | 9, 12 |
| 1586/1591/1595 | 1580 | dG | 12, 34 |
| 1655/1654/1653 | 1654 | dT C6−O6 hydrogen bond | 10 |

**Table 3. Spectral Assignment for the Most Prominent SERS Features for $d(TG_nT)$ ($n$ = 3−5) in a $K^+$ Buffer**

| SERS shift ($cm^{-1}$) $[d(TG_3T)]_4$/ $[d(TG_4T)]_4$/$[d(TG_5T)]_4$ | Raman shift ($cm^{-1}$) | assignment | refs |
|---|---|---|---|
| 1150/1151/1150 | 1180 | unpaired dT (N3) | 36 |
| 1277/1278/1275 | 1238 | dT (N3) | 36 |
| 1354/1353/1352 | 1336 | C2′ endo/anti dG | 36 |
| 1388/1389/1396 | 1363 | C2′ endo/anti dT | 36 |
| 1445/1443/1440 | 1420 | C5′ H2 | 9, 12 |
| 1509/1508/1508 | 1481 | dG N7 Hoogsten hydrogen bond | 11 |
| 1515/1514/1516 | 1490 | dG N7 hydrogen bond to $H_2O$ | 11 |
| 1598/1597/1596 | 1595 | dG N1H hydrogen bond to $H_2O$ | 12 |
| 1662/1654/1646 | 1603 | dG N1H interbase hydrogen bond | 12 |

not to the elimination of, the fluctuation of the peaks because of the previously described SERS effect. The smooth background signal, potentially due to the fluorescence contribution, could then be subtracted. Finally, spectra were smoothed and normalized to the height of the most prominent Raman peak. The right part of Figure 4 depicts the effect of $d(TG_nT)$ ($n$ = 3−5) strands in a 100 mM $K^+$ buffer. In these conditions, all of the previously mentioned GROs form quadruplex structures,[35] as verified by CD measurements. Accordingly, this leads to the appearance of characteristic features in their SERS spectra. As is possible to see, these spectra clearly resemble the spontaneous Raman scattering signal obtained by Wei et al.[36] in the analysis of parallel $[d(TG_4T)_4]$ tetramolecular G-quadruplex structures. In a comparison of the data, it is evident, however, that some features appear to have been spectrally shifted. For instance, the prominent sharp peak around 1480 $cm^{-1}$ seems to be replaced by the peak around 1508 $cm^{-1}$. Although it is impossible to exclude any form of influence from the SERS substrate on the sample structure, we believe that the observed shift is more likely attributable to the previously described SERS effect. It should be noticed that similar occurrences have been recently reported by Pagba et al.[34,37] in the investigation of the 15-mer DNA thrombin-binding aptamers, which are known to be arranged in a quadruplex structure with two G tetrads. In that case, the strong difference between the spontaneous and SERS-enhanced spectra has been attributed to the specific interaction of individual

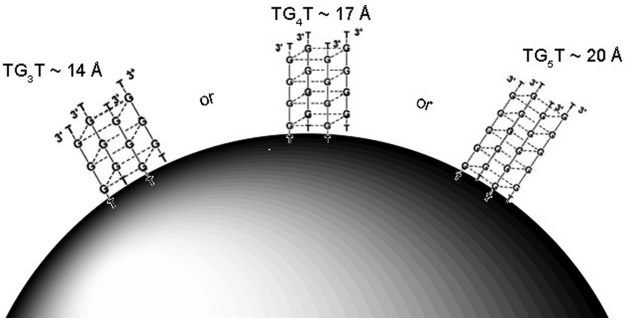


**Figure 5.** Schematic representation for the interaction between $[d(TG_3T)]_4$, $[d(TG_4T)]_4$, $[d(TG_5T)]_4$, and a silver colloidal microparticle.

vibrational modes with the metal surface. Moreover, the lack of any features in the region around 1500 $cm^{-1}$, where the C8−N7 vibration of guanine in the tetrad should occur, was ascribed to a limited exposition of the tetrads to the metallic structure, likely because of the aptamer lying flat on the metallic substrate.

In the work presented here, we observe that there is no significant spectral feature in the region below 1150 $cm^{-1}$, where vibrations of the phosphate backbone should occur,[34,37] while there is a strong enhancement of bands corresponding to vibrations of the G tetrads. These experimental features suggest, therefore, a "standing-up" orientation of $[d(TG_nT)]$ ($n$ = 3−5) in $K^+$ on the metallic surface, as shown in Figure 5. We observe for d(CTGTGTT) a relative enhancement of the Raman band around 1086 $cm^{-1}$ associated with the phosphate backbone, which indicates the proximity of backbone to the SERS substrates. Nevertheless, once more we have found that SERS spectra assume a much higher degree of reproducibility in a $K^+$ buffer (see the Supporting Information). This finding is clearly correlated to the higher order of the DNA strands.

At present, it is not possible to indicate definitively a reason for the standing-up orientation for the quadruplexes forming structures investigated in this work. However, this preferential orientation promotes the enhancement of Raman bands corresponding to intrastrand bonds, which constitutes an evident positive feature when investigating the formation of G quadruplexes. It is worth noticing that, although the SERS enhancement is particularly high for molecules that are in direct contact with the SERS substrate (the first layer effect[38]), the long-range classical electromagnetic enhancement allows the detection of signals coming from molecules within tens angstroms from the surface. In particular, for quadruplexes standing up on the SERS substrate (Figure 5), all guanine planes contribute to the SERS signal.

In Table 3, we report the assignment of the prominent peaks observed in this work for $d(TG_nT)$ with strands $n$ = 3−5 after structuration in $[d(TG_nT)]_4$. The strong band in the region around 1510 $cm^{-1}$, present for G-quadruplex structures, can be attributed to guanine ring vibrations and, as such, are quite sensitive to the N7 environment. In particular, as observed by Laporte and Thomas,[39] two contributions can be distinguished: the first due to a guanine N7 Hoogsten hydrogen bond and the second due to solvated exposed guanine N7 sites. The band around 1352 $cm^{-1}$, present in the spectra of all $d(TG_nT)$ samples annealed in a $K^+$ buffer, is attributed to deoxyguanosine sugar residues in a C2′-endo/anti, which is diagnostic of parallel quadruplex structures.[11,40] The feature around 1389 $cm^{-1}$

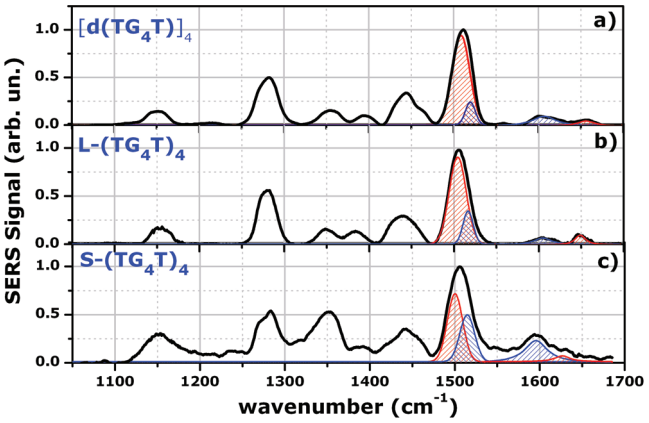


**Figure 6.** (a) Average SERS spectrum of $[d(TG_4T)]_4$, (b) *S*-$(TG_4T)_4$, and (c) *L*-$(TG_4T)_4$.

corresponds to the vibration of dT residues in a C2′ endo/anti dT conformation.[12]

Although all of the $d(TG_nT)$ samples show common features, all indicative of the parallel quadruplex structures as well as the endo/anti dT configuration, the presence of different numbers of guanine planes can be seen in the spectra of Figure 5. In particular, (i) the conformational-sensitive Raman peak around 1352 $cm^{-1}$ becomes sharper and more intense by increasing the number of G planes; (ii) the signal from the solvated H (N1) dG hydrogen bond (around 1654 $cm^{-1}$) decreases with the number of G planes, and, correspondingly, the signal of the dG N1H interbase hydrogen bond increases. Both features clearly mirror the improved stability of the $d(TG_nT)_4$ structure with the number of G planes.

**SERS Analysis of TEL Oligonucleotides.** A further step of this study was devoted to the investigation of the TEL-ODN structures. These structures, constituted by four ODN strands, whose 3′- and/or 5′-ends are attached to a non-nucleotidic branched tetra end linker, form more stable parallel G quadruplexes if compared to the corresponding tetramolecular structures.[21,41,42]

The investigation reported herein provides further insight into their structural arrangement, in relation to two specific lengths of linker residues (long L and short S). In Figure 6, we report the average SERS spectra of *L*-$(TG_4T)_4$ (trace b) and *S*-$(TG_4T)_4$ (trace c); for comparison, the spectrum corresponding to $d(TG_4T)$ in a $K^+$ buffer is also reported (trace a). Also for TEL-ODNs, the SERS features suggest a quadruplex arrangement perpendicular to the SERS substrate, as confirmed by the lack of spectral features corresponding to the alkyl chains of the TEL. Traces a and b in Figure 6, corresponding to $[d(TG_4T)]_4$ and *L*-$(TG_4T)_4$, respectively, present evident similarities. Indeed, the spectral position, as well as the relative intensities of conformational-sensitive bands, is surely comparable. Assuming that minor bands are due to residual, unpaired DNA fragments, the correspondence of the two spectra suggests that the presence of the alkyl linker does not induce a significant distortion of the phosphodiester backbone; at the same time, the strength of interaction between guanines of different strands is comparable. A more quantitative evaluation of interstrand interaction can be obtained by analyzing the relative intensity of peaks assigned to interbase hydrogen bonds with respect to the corresponding solvated hydrogen bonds. Through a fitting procedure, we evaluated the ratio $R_1 = I_{1508}/I_{1514}$ between Raman peaks at 1508 and 1514 $cm^{-1}$ as well as the ratio $R_2 = I_{1654}/I_{1597}$ between Raman peaks at 1654 and 1597 $cm^{-1}$. In fact, as reported in Table 3, peaks at 1508 and 1654 $cm^{-1}$ are due to Hoogsten hydrogen bonds (indicating the strong interaction between the different guanines), while peaks at 1514 and 1597 $cm^{-1}$ are due to the corresponding solvated hydrogen bonds (indicating the much weaker interaction between guanines and solvent). The obtained results are reported in Table 4. As is possible to see, *L*-$(TG_4T)_4$ and $[d(TG_4T)]_4$ spectra present quite similar low $R_1$ values, while the $R_2$ value suggests a higher stability for the first structure.

**Table 4. Ratio $R_1 = I_{1508}/I_{1514}$ and $R_2 = I_{1654}/I_{1597}$, As Obtained by the Fitting Procedure[a]**

| | $[d(TG_4T)]_4$ | *L*-$(TG_4T)_4$ | *S*-$(TG_4T)_4$ |
|---|---|---|---|
| $R_1$ | 3.5 ± 0.4 | 3.2 ± 0.3 | 1.4 ± 0.2 |
| $R_2$ | 0.42 ± 0.05 | 0.77 ± 0.09 | 0.20 ± 0.04 |

[a] The reported errors represent the standard deviation values derived from independently prepared samples.

A quite different conclusion can be reached in the case of *S*-$(TG_4T)_4$ spectra (trace c in Figure 6). In this case, a relatively strong spectral feature at 1514 $cm^{-1}$ can be observed, which leads to $R_1 = 0.7$. Additionally, the two Raman peaks in the spectral region between 1590 and 1660 $cm^{-1}$ seem to collapse in only one broad feature centered around 1590 $cm^{-1}$ with only a wing at ∼1660 $cm^{-1}$. We speculate that the broad peak is due to hydrogen bonds from different environments with a major contribution from solvated hydrogen bonds. The comparison of traces a and c discloses further differences in the region around 1396 $cm^{-1}$. In this region, it is immediately obvious that the relative intensity of the dT-sensitive peak is strongly reduced with respect to the $[d(TG_4T)]_4$ spectrum, providing evidence of deformation for the phosphodiester backbone.

Putting together all of the observed features, it is possible to speculate on the effective structural conformation of *L*-$(TG_4T)_4$. We hypothesize that, different from what happens for *L*-$(TG_4T)_4$, the shorter TEL induces a slight distortion in the glycosylic backbone and, eventually, also a G-plane instability. In particular, it is reasonable to suggest that the first G plane, opposite to the arms of the linker, becomes less stable and only poorly stacked to the adjacent G-tetrad plane. Possibly, glycosylic backbone distortion could even lead to the complete distruption of G-tetrad interstrand connections, with the consequent opening of the last guanine plane, as confirmed by the presence of the peak at 1590 $cm^{-1}$, due to hydrated N1H bonds.

## CONCLUSIONS

SERS from silver nanoparticles has been shown to be a quantitative analytical technique to investigate the formation and to analyze the relative strength of G quadruplexes. The results presented demonstrate that, in a $K^+$ buffer, quadruplexes tend to adopt a perpendicular or "standing-up" orientation with respect to the silver colloidal substrate, therefore exposing the guanine tetrad to the metallic surface. In doing so, this produces a favorable configuration for investigating the intrastrand bonding. Furthermore, we systematically analyzed the SERS signal fluctuations before and after structuring in the G quadruplex, observing a great enhancement of the signal reproducibility in the second case. Importantly, we demonstrated, for the first time, that SERS

can be used to analyze the relative stability of G-quadruplex structures with different numbers of G planes. We believe that our experimental outcomes firmly demonstrate that SERS-based assays can be used in providing new information on the quadruplex formation from single DNA strands.

## ■ ASSOCIATED CONTENT

**Supporting Information.** Synthesis of DNA, the formation of G-quadruplex structures, CD details, experimental setup, and analysis of SERS spectra fluctuations. This material is available free of charge via the Internet at http://pubs.acs.org.

## ■ AUTHOR INFORMATION

### Corresponding Authors

*E-mail: giulia.rusciano@na.infn.it (G.R.), golivier@unina.it (G.O.).

## ■ ACKNOWLEDGMENT

The authors thank Dr. R. Marchington for the critical reading of the manuscript. A.C.D.L. is an EPSRC research fellow.

## ■ REFERENCES

(1) Chang, C.; Kuo, I.; Ling, I.; Chen, C.; Chen, H.; Lou, P.; Lin, J.; Chang, T. *Anal. Chem.* **2004**, *76*, 4490–4494.
(2) Chang, C.; Chu, J.; Kao, F.; Chiu, Y.; Lou, P.; Chen, H.; Chang, T. *Anal. Chem.* **2006**, *78*, 2810–2815.
(3) Lipps, H.; Rhodes, D. *Trends Cell Biol.* **2009**, *19*, 414–422.
(4) Basnar, B.; Elnathan, R.; Willner, I. *Anal. Chem.* **2006**, *78* 3638–3642.
(5) Oliviero, G.; Amato, J.; Borbone, N.; D'errico, S.; Galeone, A.; Mayol, L.; Haider, S.; Olu-biyi, O.; Hoorelbeke, B.; Balzarini, J.; Piccialli, G. *Chem. Commun.* **2010**, *46*, 8971–8973.
(6) Li, T.; Wang, E.; Dong, S. *Anal. Chem.* **2010**, *82*, 7576–7580.
(7) David, W.; Brodbelt, J.; Kerwin, S.; Thomas, P. *Anal. Chem.* **2002**, *74*, 2029–2033.
(8) Lyon, L.; Keating, C.; Fox, A.; Baker, B.; He, L.; Nicewarner, S.; Mulvaney, S.; Natan, M. *Anal. Chem.* **1998**, *70*, 341R–361R.
(9) Benevides, J.; Kang, C.; Thomas, G. *Biochemistry* **1996**, *35* 5747–5755.
(10) Wei, C.; Jia, G.; Yuan, J.; Feng, Z.; Li, C. *Biochemistry* **2006**, *45*, 6681–6691.
(11) Miura, T.; Thomas, G. *Biochemistry* **1994**, *33*, 7848–7856.
(12) Krafft, C.; Benevides, J.; Thomas, G. *Nucleic Acids Res.* **2002**, *30*, 3981–3991.
(13) Kneipp, K.; Kneipp, H.; Itzkan, I.; Dasari, R.; Feld, M. *Chem. Rev.* **1999**, *99*, 2957–76.
(14) Kneipp, K.; Kneipp, H.; Itzkan, I.; Dasari, R.; Feld, M. *J. Phys.: Condens. Matter* **2002**, *14*, R597–R624.
(15) Kneipp, K.; Kneipp, H.; Kartha, V.; Manoharan, R.; Deinum, G.; Itzkan, I.; Dasari, R.; Feld, M. *Phys. Rev. E* **1998**, *57*, R6281–R6284.
(16) Hu, J.; Zhang, C. *Anal. Chem.* **2010**, *82*, 8991–8997.
(17) Zhang, H.; Harpster, M. H.; Park, H. J.; Johnson, P. A. *Anal. Chem.* **2011**, *83*, 254–260.
(18) Barhoumi, A.; Zhang, D.; Halas, N. J. *J. Am. Chem. Soc.* **2008**, *130*, 14040–14041.
(19) Breuzard, G.; Millot, J.; Riou, J.; Manfait, M. *Anal. Chem.* **2003**, *75*, 4305–4311.
(20) Oliviero, G.; Borbone, N.; Galeone, A.; Varra, M.; Piccialli, G.; Mayol, L. *Tetrahedron Lett.* **2004**, *45*, 4869–4872.
(21) Oliviero, G.; Borbone, N.; Amato, J.; D'Errico, S.; Galeone, A.; Piccialli, G.; Varra, M.; Mayol, L. *Biopolymers* **2009**, *91*, 466–477.
(22) De Luca, A. C.; Rusciano, G.; Caserta, S.; Guido, S.; Sasso, A. *Macromolecules* **2008**, *41*, 5512–5514.
(23) Lee, P.; Meisel, D. *J. Phys. Chem.* **1982**, *86*, 3391–3395.
(24) Kitahama, Y.; Tanaka, Y.; Itoh, T.; Ozaki, Y. *Phys. Chem. Chem. Phys.* **2010**, *12*, 7457–7460.
(25) Le Ru, E. C.; Etchegoin, P. G. *Chem. Phys. Lett.* **2004**, *396* 393–397.
(26) Creighton, J.; Baucom, K. *Surf. Sci.* **1998**, *409*, 372–383.
(27) Panicker, C. Y.; Varghese, H. T.; Anto, P. L.; Philip, D. *J. Raman Spectrosc.* **2006**, *37*, 853–857.
(28) Gao, X.; Davies, J.; Weaver, M. *J. Phys. Chem.* **1990**, *94* 6858–6864.
(29) Moskovits, M.; SUH, J. *J. Phys. Chem.* **1988**, *92*, 6327–6329.
(30) Topacli, A.; Kesimli, B. *Spectrosc. Lett.* **2001**, *34*, 513–526.
(31) Gearheart, L.; Ploehn, H.; Murphy, C. *J. Phys. Chem. B* **2001**, *105*, 12609–12615.
(32) Brabec, V.; Niki, K. *Biophys. Chem.* **1985**, *23*, 63–70.
(33) Jain, A.; Murty, M.; Flynn, P. *ACM Comput. Surveys (CSUR)* **1999**, *31*, 264–323.
(34) Pagba, C. V.; Lane, S. M.; Wachsmann-Hogiu, S. *J. Raman Spectrosc.* **2010**, *41*, 241–247.
(35) Gros, J.; Rosu, F.; Amrane, S.; Cian, A. D.; Gabelica, V.; Lacroix, L.; Mergny, J. *Nucleic Acids Res.* **2007**, *35*, 3064.
(36) Wei, C.; Jia, G.; Yuan, J.; Feng, Z.; Li, C. *Biochemistry* **2006**, *45*, 6681–6691.
(37) Pagba, C. V.; Lane, S. M.; Cho, H.; Wachsmann-Hogiu, S. *J. Biomed. Opt.* **2010**, *15*, 047006.
(38) Mrozek, I.; Otto, A. *Europhys. Lett.* **1990**, *11*, 243.
(39) Laporte, L.; Thomas, J. *J. Mol. Biol.* **1998**, *281*, 261–270.
(40) Miura, T.; Thomas, G. *Biochemistry* **1995**, *34*, 9645–9654.
(41) Oliviero, G.; Amato, J.; Borbone, N.; Galeone, A.; Varra, M.; Piccialli, G.; Mayol, L. *Bioconjugate Chem.* **2006**, *17*, 889–898.
(42) Oliviero, G.; Amato, J.; Borbone, N.; Galeone, A.; Varra, M.; Piccialli, G.; Mayol, L. *Biopolymers* **2006**, *81*, 194–201.